

# Simulation of transient current through PMMA thin films based on a random walk model

A. Hacinliyan

*Department of Physics, Yeditepe University, Kayisdagi Caddesi, 34755 Kadikoy, Istanbul, Turkey*

Y. Skarlatos and H. A. Yildirim

*Department of Physics, Bogazici University, 34342 Bebek, Istanbul, Turkey*

G. Sahin\*

*Department of MIS, Yeditepe University, Kayisdagi Caddesi, 34755 Kadikoy, Istanbul, Turkey*

(Received 24 September 2005; revised manuscript received 13 January 2006; published 27 April 2006)

A piecewise continuous, time dependent diffusive coupling in a classical one-dimensional randomly pinned charge density wave model has been used for the analysis of experimentally observed transient current data for polymethyl methacrylate. Satisfactory agreement has confirmed that this can be a dynamical model for the behavior of the transient current. The analysis also suggests the presence of three different regimes in the decay of the transient current.

DOI: [10.1103/PhysRevB.73.134302](https://doi.org/10.1103/PhysRevB.73.134302)

PACS number(s): 75.40.Gb, 75.40.Mg, 73.50.Gr

## I. INTRODUCTION

Polymeric dielectrics have complicated structures that may contain many impurities and additives. They are also known to be very sensitive to their thermal, mechanical, and electrical history.<sup>1-4</sup> The difficulty of obtaining identical results under nearly identical conditions has been reported in the literature.<sup>2</sup>

Polar polymers such as polymethylmethacrylate (referred to as PMMA in the rest of this work), are known to need very long times to reach a steady state current. From theoretical considerations,<sup>1</sup> this time has been estimated to be approximately a 100 years for PMMA. In spite of the dependence on the history, experimentally observed reproducible chaotic behavior as reflected by a positive Liapunov exponent in the transient current has been reported.<sup>5,6</sup>

In order to furnish a theoretical interpretation to the observations, a classical one-dimensional model of randomly pinned charge density waves (CDW) is proposed.<sup>7</sup> The aim is to understand the experimentally observed decaying transient current as a time dependent dynamical system based on this model. There are three reasons behind this choice: (i) the qualitative resemblance of the observed decaying patterns of the current, and simulations based on this model; (ii) the observation of a positive Lyapunov exponent in the data which also agrees with the model; (iii) the similarity of the observed electric field dependence of conductivity with this model.<sup>6,8</sup>

History dependence is also known to be a property of spin glasses, polymers,<sup>9</sup> as well as processes described by a continuous time random walk.<sup>10,11</sup> The proposed model inherits glassy dynamics, is akin to the short-range Ising spin glass, and can describe random walks on directed percolation clusters.<sup>8</sup> All of these systems show memory effects. Another reason for the choice of the model is that it makes use of quenched randomness, which accounts for the heterogeneity of the polymer and reflects nonlinearity in the transient current.

The experimental setup is briefly summarized in Sec. II. The model is described in Sec. III. The simulation process is

presented in Sec. IV. Our results are discussed in Sec. V.

## II. EXPERIMENT

The specimens under study were prepared as sandwiched metal-polymer-metal structures with PMMA as the isolating layer. 300 nm thick aluminum electrodes were thermally evaporated at  $10^{-6}$  mbar on microscope glass slides cleaned in a detergent solution. 20  $\mu\text{m}$  thick PMMA layers were deposited from 6% PMMA solution in toluene. Subsequently, aluminum top contacts were evaporated. The  $I$ - $V$  measurement was performed via a programmable picoammeter and/or voltage source (Keithley, model 487) and a temperature controller (Lake Shore, model 300). Cyro industries model DET has been used as a sample holder. The picoammeter and the temperature controller were interfaced to a computer through an interface card that automated data taking. Details are reported in Ref. 5.

## III. MODEL

The overdamped equation of motion for the phase  $\phi_i$  of a pinned CDW is given by<sup>7</sup>

$$-\frac{K}{q_0^2} \frac{\partial^2 \phi}{\partial x^2} - \frac{\rho_m}{q_0^2 \tau_0} \sum_j \dot{\phi} \delta(x - x_j) + eCV_0 \rho_0 \sum_j \sin[q_0 x_j + \phi(x)] \delta(x - x_j) + \frac{e\rho_0}{q_0} E = 0, \quad (1)$$

where  $C = cN_0\Delta/a\lambda\rho_0$ ,  $N_0$  is the constant density of states per site,  $a$  is the lattice constant,  $\Delta$  the gap,  $\lambda$  the electron phonon coupling,  $l = 2\pi/q_0$  the wavelength,  $\rho_0$  the one-dimensional electron density,  $\rho_m$  the effective mass density of the charge density wave, and  $V_0$  the intensity of the interaction of the charge density wave with the local impurities whose densities are  $n_i$ .  $K = \rho_0 m v_f^2$  with  $m$  the free electron mass and  $v_f$  the Fermi velocity and  $\tau$  is a phenomenological parameter describing the dissipation of energy from the

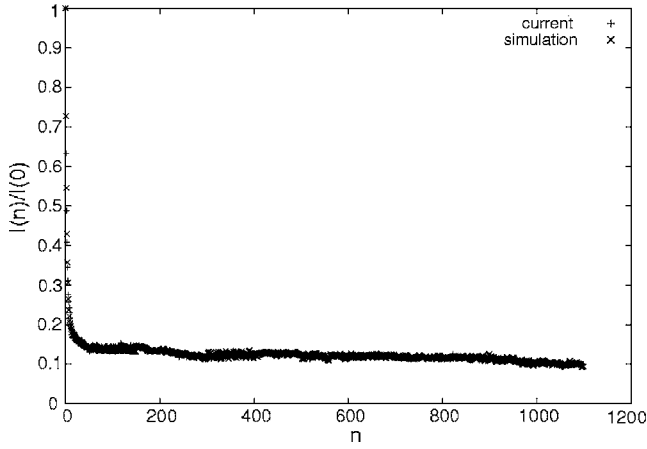


FIG. 1. CDW fit of current at 3.25 MV/m. Both the measured current (+) and simulated CDW polarization current (×) are normalized and drawn versus the number of time steps ( $n$ ).

charge density wave to the lattice. The above equation of motion can be replaced by a difference equation and the latter can be integrated between any two consecutive impurity sites and reduces to a difference equation.

Introducing the dimensionless variables  $u = n_i x$ ,  $\xi = E / CV_0 n_i q_0$ ,  $B = 2\pi K n_i / CV_0 \rho_0 q_0^2$ ,  $s = t / \tau_0$ , where  $\tau_0 = 2\pi \rho_0 m n_i^2 / CV_0 \rho_0 q_0 \tau$  and  $\psi = \phi(x) / 2\pi$  and  $Q_0 = q_0 / 2\pi n_i$  the difference equation becomes

$$\frac{d\psi_j}{ds} = B \left[ \frac{\psi_{j+1} - \psi_j}{r_{j+1,j}} - \frac{\psi_j - \psi_{j-1}}{r_{j,j-1}} \right] - \sin[2\pi(u_j Q_0 + \psi_j)] + \xi Q_j, \quad (2)$$

where  $Q_j = \frac{1}{2}(r_{j+1,j} + r_{j,j-1})$ ,  $j \geq 1$ . If one introduces the quenched random variable  $\phi_j = u_j Q_0$ ,  $1 \leq \phi_j \leq 1$ , and takes the intervals between the impurity sites to be uniform the equation of motion becomes

$$\frac{d\psi_j}{ds} = B[\psi_{j+1} + \psi_{j-1} - 2\psi_j] - \sin[2\pi(\phi_j + \psi_j)] + \xi, \quad (3)$$

where the dimensionless constants  $\xi$  and  $B$  correspond to the electric field and to the diffusive coupling, respectively. In terms of  $\psi_j$  the current density is given by

$$J = en_e \frac{2\pi}{q_0 \tau_0} \left\langle \frac{d\psi_j}{ds} \right\rangle, \quad (4)$$

where  $n_e$  is the bulk density and  $\langle \rangle$  represents an average over all impurity sites.

This is a classical one-dimensional model that studies the overdamped phase dynamics of CDW pinned by randomly located impurities. Two of the most important results of the model<sup>7</sup> are a resulting nonlinear polarization current and the existence of both broad and narrow band noise in the polarization current.<sup>8</sup> For these reasons we attempted to base our understanding of the experimentally observed transient current in PMMA on this CDW model.<sup>6</sup>

Another point of concern is the chaotic nature of the coupled lattice maps, of which Eq. (3) is an example<sup>8</sup>. The existence of a maximal positive Lyapunov exponent in the

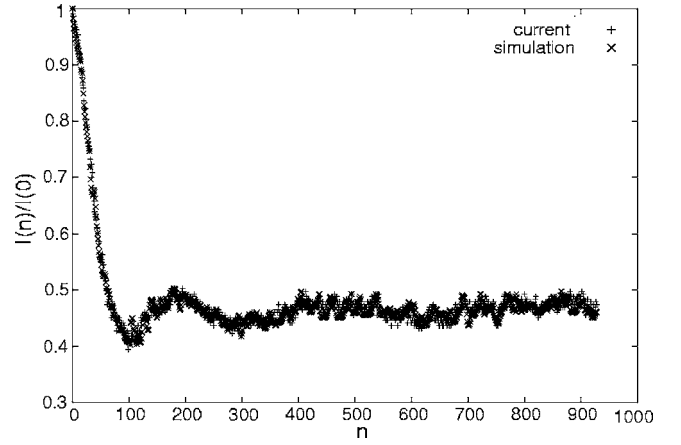


FIG. 2. CDW fit of a current at 2.50 MV/m [current (+), simulation (×)].

transient current through PMMA<sup>6</sup> and the similar behavior of the polarization current in the model is another factor for using the model in simulation of the transient current.

#### IV. SIMULATION

The competition between the quenched random field and the elastic restoring forces invokes some very complex dynamics. Charge density waves provide one of the very few cases where it is possible to study the effects of quenched randomness due to impurities in such systems.

The recursion relation given by Eq. (3) is used as the CDW model. It is numerically simulated, and with the use of evaluated values of phases, the polarization current has been computed.

The simulated model has then been fitted to the experimentally observed transient current through PMMA. The simulation and the fitting codes are written in the Fortran programming language. The data and the simulation for the transient current are normalized between 0 and 1. There are four parameters, the number of the impurity sites, the number of time steps, the values of  $B$  and  $\xi$  that control the behavior of the CDW polarization current. Initial conditions are chosen randomly, that is, the code fills the initial values of the impurity sites with quenched random values which have values between 0 and 1.  $N$  (the number of time steps), the number of states (which is set to 10 000 as in Ref. 8) are given manually to the code. Of the two parameters,  $\xi$  represents the forcing electric field and  $B$  represents the diffusive coupling. A constant value for the former fits the experimental data satisfactorily.

For a satisfactory fit,  $B$  has to be taken as a time dependent parameter. For simplicity, the following approach is used. The data are split into time intervals of the order of the first minimum of the average mutual information function given by

$$S = - \sum_{ij} p_{ij}(\tau) \ln \frac{p_{ij}(\tau)}{p_i p_j}. \quad (5)$$

Here  $p_i$  is the probability of finding a data value in the  $i$ th interval.  $p_{ij}(\tau)$  is the joint probability of data to be in the  $i$ th

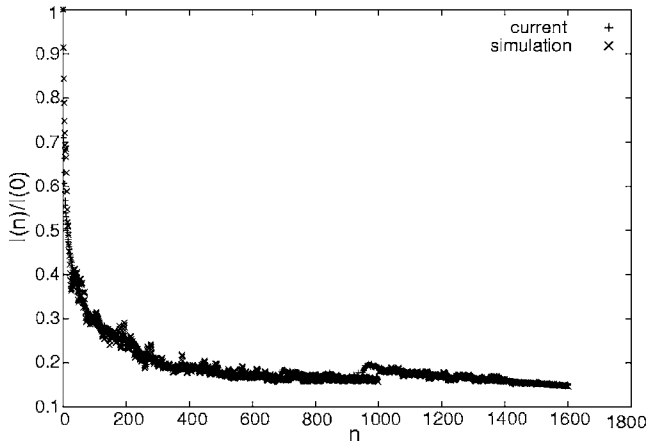


FIG. 3. CDW fit of a current at 2.0 MV/m [current (+), simulation (x)].

interval first, and  $\tau$  times later in the  $j$ th interval. This is evaluated for the experimental data by the Tisean package.<sup>13</sup> Mutual information gives an estimate for the information connection between data values. The CERN MINUIT package<sup>12</sup> is used to find the best fit for an overall  $\xi$  and  $B$  for each interval.

Figures 1–3 show the simulation and the data for an applied voltage of 3.25 MV/m, 2.50 MV/m, and 2.0 MV/m, respectively.

The fit required three different constant values for the parameter  $B$  for different regions of time. In order to verify this observation that more than one different region of  $B$  is indicated, detrended fluctuation analysis (DFA) is used on the observed time series,<sup>14,15</sup> assuming that a change in the dynamics of the system would involve a change in the pinning and hence  $B$ . DFA is a scaling analysis method used to estimate long-range power-law correlation exponents.<sup>16–18</sup> One integrates the time series of length  $N$ , then divides the result into boxes of equal length,  $n$ . In each box of length  $n$ , a least squares line is fit to the data. The  $y$  coordinate of the straight line segments is denoted by  $y_n(k)$ . Next, the integrated time series  $y(k)$  is detrended, by subtracting the local

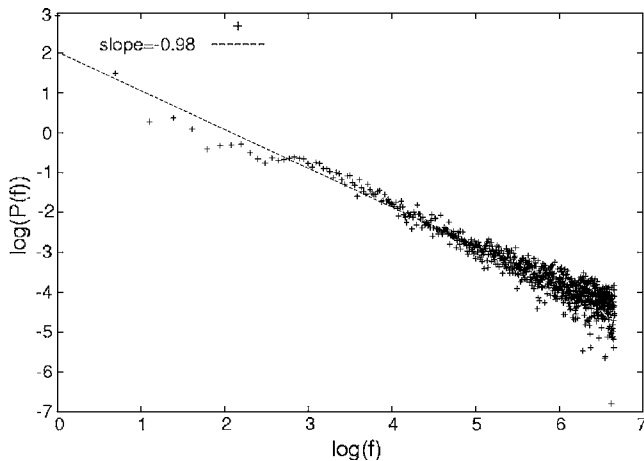


FIG. 4. Power spectrum analysis of the observed current at 2 MV/m. The slope of the straight line is equal to  $-0.98$ .

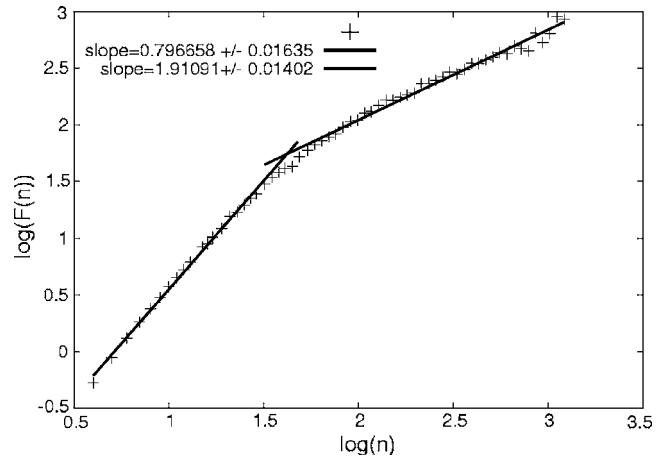


FIG. 5. Plot of  $\log F(n)$  vs  $\log n$  for the time series of the  $x$  component of Lorenz equations showing the crossover.

trend,  $y_n(k)$ , in each box. The root-mean-square fluctuation of this integrated and detrended time series is calculated by

$$F(n) = \sqrt{\frac{1}{N} \sum_{k=1}^N [y(k) - y_n(k)]^2}. \quad (6)$$

This computation is repeated over all time scales (box sizes) to characterize the relationship, between  $F(n)$ , the average fluctuation, as a function of box size  $n$  (see Figs. 4 and 5). A linear relationship on a log-log plot indicates the presence of power-law scaling. Under such conditions, the fluctuations can be characterized by a scaling exponent,  $\alpha$ , such that  $F(n) \sim n^\alpha$ . A crossover in the scaling exponent,  $\alpha$ , indicates a transition from one type to a different type of underlying correlations, due to a transition in the dynamical properties.<sup>16,17</sup>

Figures 6–8 show  $\log[F(n)]$  vs  $\log(n)$  for 3.25 MV/m, 2.50 MV/m, and 2.0 MV/m, respectively, both for the current and the simulation. Although a precise identification of the power-law behavior would require more decades of data,

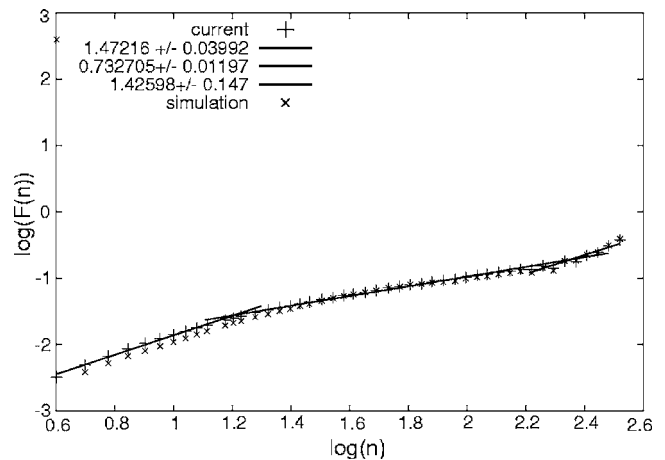


FIG. 6.  $\log[F(n)]$  vs  $\log(n)$  with three different scaling exponents for the measured current (+) at 3.25 MV/m and the simulation (x). The inset show the scaling exponents for the current.

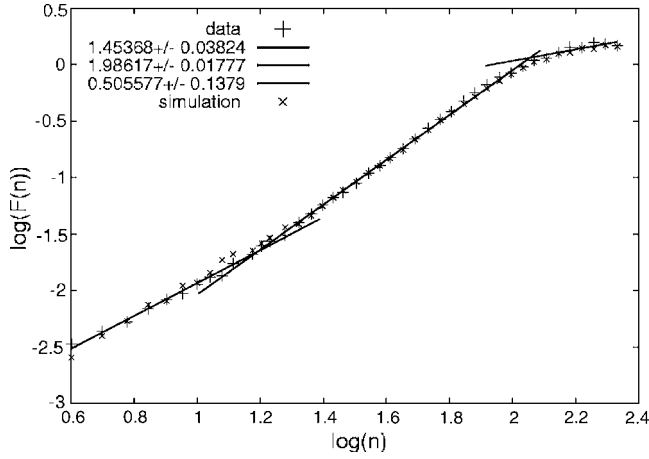


FIG. 7.  $\log[F(n)]$  vs  $\log(n)$  with three different scaling exponents for the measured current (+) at 2.50 MV/m and the simulation. The inset show the scaling exponents for the current.

a discontinuity in slopes clearly indicates three regions for the 3.25 MV/m data. Although a linear log-log plot is less clearly indicated for a large box size for the next lowest voltage of 2.50 MV/m, three regions can still be identified. In this set one can observe a middle region with a slope nearly equal to 2 followed by a crossover, which, according to Refs. 16 and 19 might be caused by a sinusoidal trend rather than a change in the dynamical properties of the system. The similarity between the crossover regions in the data and the simulation leads us to conclude that the crossover is more likely to result from a transition in the dynamical properties of the system. The process under study is basically diffusive and damped with chaotic fluctuations; the pinning parameter  $B$  is indirectly related to the damping because of the scaled timelike parameter in the CDW model used in this work. Moreover, in Ref. 6, this data set is reported to have the minimum maximal Lyapunov exponent with respect to other data sets, which might explain why this data set (Fig. 2) seems to be more periodiclike than other sets. The power spectrum for the 2.0 MV/m data shown in Fig. 4 does not show any marked indication of periodic behavior. One can also see a crossover behavior from a region with a slope near 2 similar to that in the data when the DFA analysis is applied to a numerical solution of Lorenz equations. This is shown in Fig. 5. For the lowest voltage of 2.0 MV/m the demarcation of regions is less clear but plausible.

Table I summarizes the results of the fit and the DFA scaling exponents. The three different regions with the corresponding values of  $B$  and the values for the scaling exponents are shown. The variation of the scaling exponent at the weakest applied electric field among regions is less pro-

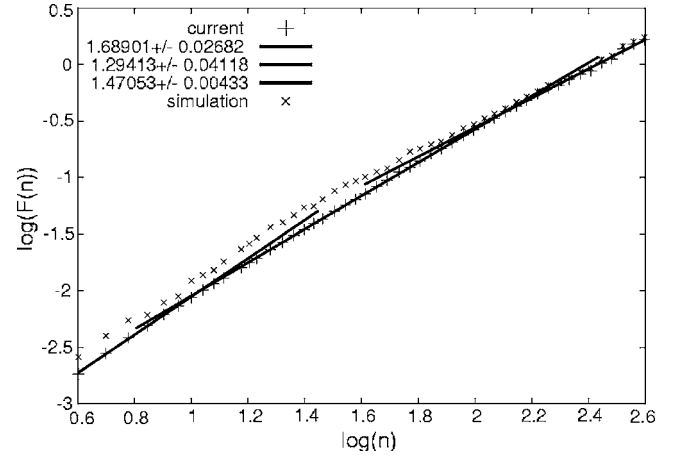


FIG. 8.  $\log[F(n)]$  vs  $\log(n)$  with three different scaling exponents for the measured current (+) at 2.00 MV/m and the simulation (x). The inset shows the scaling exponents for the current.

nounced. For stronger applied electric fields, the values of  $B$  for the first two regions seem to show a significantly slower variation, but attempting a single overall value deteriorates the fit. It is also observed that as the voltage increases the long-range correlations (indicated by  $\alpha$ ) decrease, and the regime changes become more distinct. This behavior seems to be consistent with the strong dependence of conductivity on the electric field.<sup>2</sup> The field dependence is mostly attributed to the trapping of free charge carriers in the volume of the dielectric during their motion due to the applied field, whereas the release from traps was considered to be thermally activated with a field-modified activation energy.<sup>20</sup> These charges are believed to be trapped in some of the pinning states arising from the defects in the structure of the insulator such as impurities, dopants, and dangling bonds. It has been suggested that side groups may act in a way similar to doped impurities.<sup>21</sup> The variation of  $B$  seems to be related to the competition between the mechanisms of conductivity in PMMA via dipole relaxation processes, caused by heterogeneities and the trapping of charge carriers.<sup>2</sup> It is known that dipole relaxation completes before other mechanisms.<sup>22</sup> This is probably related to the first crossover in the scaling exponent. The other two crossovers in  $\alpha$  might be due to a relaxation caused by heterogeneities and the trapping of charge carriers.

## V. DISCUSSION

In this work, an attempt has been made to simulate the experimentally observed polarization decay current in terms of a dynamical system with a diffusive coupling that is piece-

TABLE I. The scaling exponents, the  $B$  values, and the  $\xi$  values for the three applied electric fields.

	$\alpha_1$	$\alpha_2$	$\alpha_3$	$B_1$	$B_2$	$B_3$	$\xi$
3.25 MV/m	1.47	0.73	1.43	$1.3 \pm 0.2$	$1.4 \pm 0.2$	$1.3 \pm 0.2$	0.7
2.50 MV/m	1.45	1.98	0.5	$1.3 \pm 0.1$	$1.4 \pm 0.1$	$1.7 \pm 0.1$	0.53
2.0 MV/m	1.69	1.47	1.3	$0.8 \pm 0.05$	$0.7 \pm 0.05$	$0.8 \pm 0.05$	0.62

wise continuous in time. The discontinuities indicate the presence of three different time dependent nonlinear conductivity mechanisms. This presence is supported by a detrended fluctuation analysis. An overall positive Lyapunov exponent had been observed and reported elsewhere.<sup>5,6</sup> An attempt has been made to model the indicated chaotic behavior in terms of a model describing pinned charge density waves. Charge density waves have been reported in certain polymers,<sup>23</sup> but not yet in PMMA. A satisfactory fit to the model has been obtained, however it is not absolutely clear whether this is a pure charge density wave effect, or there are further interactions which can still be modeled by the CDW model by admitting a piecewise time dependent diffusive coupling.

Piecewise time dependence agrees with the DFA results. One reason for the time dependence of the diffusive coupling may be aging under the influence of the applied electric field (for aging effects in PMMA see Refs. 1 and 3). The continued application of an electric field is affecting the configuration of the polymer. Thus the heavily pinned charge density wave model stands as a good candidate for modeling the transient current.

#### ACKNOWLEDGMENT

We wish to thank Ayşe Erzan for her suggestions and encouragement.

---

\*Also at Department of Physics, Bogazici University, 34342 Bebek, Istanbul, Turkey.

<sup>1</sup>K. Mazur, *J. Phys. D* **30**, 1383 (1997).

<sup>2</sup>V. Adamec and J. H. Calderwood, *J. Phys. D* **11**, 781 (1978).

<sup>3</sup>S. Boettcher and M. Paczuski, *Phys. Rev. Lett.* **79**, 889 (1997).

<sup>4</sup>L. Bellon, S. Ciliberto, and C. Laroche, *Europhys. Lett.* **51**, 551 (2000).

<sup>5</sup>A. Hacinliyan, Y. Skarlatos, G. Sahin, and G. Akin, *Chaos, Solitons Fractals* **17**, 575 (2003).

<sup>6</sup>A. Hacinliyan, Y. Skarlatos, H. A. Yildirim, and G. Sahin, *Fractals* (to be published June 2006).

<sup>7</sup>L. Pietronero and S. Strassler, *Phys. Rev. B* **28**, 5863 (1983).

<sup>8</sup>A. Erzan, E. Veermans, R. Heijungs, and L. Pietronero, *Phys. Rev. B* **41**, 11522 (1990).

<sup>9</sup>P. Allegrini, G. Aquino, P. Grigolini, L. Palatella, A. Rosa, and B. J. West, *Phys. Rev. E* **71**, 066109 (2005).

<sup>10</sup>E. Barkai, *Phys. Rev. Lett.* **90**, 104101 (2003).

<sup>11</sup>P. Allegrini, G. Aquino, P. Grigolini, L. Palatella, and A. Rosa, *Phys. Rev. E* **68**, 056123 (2003).

<sup>12</sup>F. James and M. Roos, *Comput. Phys. Commun.* **10**, 343 (1975); CERN library program D506.

<sup>13</sup>R. Hegger, H. Kantz, and T. Schreiber, *Chaos* **94**, 413 (1999).

<sup>14</sup>C. K. Peng, S. V. Buldyrev, S. Havlin, M. Simons, H. E. Stanley,

and A. L. Goldberger, *Phys. Rev. E* **49**, 1685 (1994).

<sup>15</sup>C. K. Peng, S. Havlin, H. E. Stanley and A. L. Goldberger, *Chaos* **5**, 82 (1995).

<sup>16</sup>K. Hu, P. Ch. Ivanov, Z. Chen, P. Carpena, and H. E. Stanley, *Phys. Rev. E* **64**, 011114 (2001).

<sup>17</sup>Z. Chen, P. Ch. Ivanov, K. Hu, and H. E. Stanley, *Phys. Rev. E* **65**, 041107 (2002).

<sup>18</sup>A. L. Goldberger, L. A. N. Amaral, L. Glass, J. M. Hausdorff, P. Ch. Ivanov, R. G. Mark, J. E. Mietus, G. B. Moody, C.-K. Peng, and H. E. Stanley, *PhysioBank, PhysioToolkit, and PhysioNet: Components of a New Research Resource for Complex Physiologic Signals. Circulation* 101(23): e215-e220 [Circulation Electronic Pages; <http://circ.ahajournals.org/cgi/content/full/101/23/e215>]; 2000 (June 13).

<sup>19</sup>Z. Chen, K. Hu, P. Carpena, P. Bernaola-Galvan, H. E. Stanley, and P. Ch. Ivanov, *Phys. Rev. E* **71**, 011104 (2005).

<sup>20</sup>T. J. Lewis, *J. Phys. D* **23**, 1469 (1990).

<sup>21</sup>A. Heuer and P. Neu, *J. Chem. Phys.* **107**, 8686 (1997).

<sup>22</sup>J. Sorensan, *Engineering Tools for Internal Charging, European Space Agency, DERA/CIS/CIS2/CR000277* issue 1.0 (2000).

<sup>23</sup>K. L. Yao, S. E. Han, and L. Zhao, *J. Chem. Phys.* **114**, 6437 (2001).